



Determining the transmission loss of apertures above the plane wave cutoff frequency

Jiazhu LI¹; Jian CHEN²; Can LI³

¹ Institute of Sound and Vibration Research, Hefei University of Technology, China

² Institute of Sound and Vibration Research, Hefei University of Technology, China

³China Automotive Technology & Research Center, China

ABSTRACT

In order for enclosures and barriers to be effective, the sound transmission through holes and openings must be minimized. In this paper, a modal and sound transmission coefficient superposition (MSTCS) method is used to predict the sound transmission loss (TL) of apertures. The approach is applicable both below and above the cutoff frequency and may be used for apertures of arbitrary cross-section. Rectangular cross-section openings are considered and results are compared with the transfer matrix method, Sgard et al., acoustic FEM, and published experimental data and demonstrate good agreement with each other.

Keywords: Transmission Loss, Apertures

1. INTRODUCTION

Leaks and openings are common in both enclosures and barriers. It is well known that the presence of openings will significantly diminish the performance of an enclosure (1). Often, apertures are unavoidable because they are needed for wiring, thermal reasons, or air circulation. Moreover, there are often slits or gaps between on the edges of access doors or windows. The transmission loss through an aperture can often be increased by lengthening the aperture or leak (2-4). Indeed, lengthening is often the only alternative.

A number of investigators have examined the impact of apertures. Gomperts (2), Gomperts and Kihlman (5), Wilson and Soroka (6), and Sauter and Soroka (7) developed expressions for circular and rectangular apertures. Mechel (3) included the effects of both sealing and absorption in the aperture. The authors used a transfer matrix approach to determine the transmission loss of apertures (4). In each of the aforementioned papers, plane wave propagation was assumed in the aperture

Sgard et al. (8) reviewed the prior work and developed a general equation for larger apertures with uniform cross-section including higher order wave behavior. Trompette et al. (9) measured the transmission loss for large openings and results were compared to the model developed by Sgard et al. (8) with good agreement. Sieck et al. (10) determined the insertion loss of an aperture in an enclosure in a manner similar to Sgard et al. (8). Jordi and Antonio (11) developed a modal based approach to predict the sound transmission of apertures between cuboid-shape rooms.

In this paper a modal and sound transmission coefficient superposition (MSTCS) method to predict the transmission loss of large apertures is developed. The approach is similar to Sgard et al. (8) but is more efficient. Results are compared with the authors' prior work (4), Sgard et al. (8), Trompette et al. (9) and an acoustic FEM method detailed in Reference (12-15) and implemented in the ESI VA-One software (16).

2. MODAL and SOUND TRANSMISSION COEFFICIENT SUPERPOSITION

¹ Jiazhu.li@hotmail.com

² hfgd_8216@126.com

³ lican1207@163.com

APPROACH

2.1 Basic Theories (17)

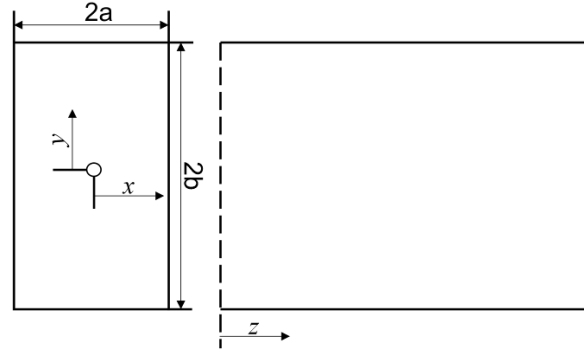


Figure 1 – Schematic Representation of Rectangular Aperture

Figure 1 shows a schematic representation of a rectangular aperture. The three dimensional wave equation can be expressed as

$$\left[\frac{\partial^2}{\partial t^2} - c_0^2 \nabla^2 \right] = 0 \quad (1)$$

For a rectangular aperture, the the solution to the wave equation is given as

$$p(x, y, z, t) = (C_1 e^{-jk_z z} + C_2 e^{+jk_z z}) (e^{-jk_x x} + C_3 e^{+jk_x x}) (e^{-jk_y y} + C_4 e^{+jk_y y}) e^{j\omega t} \quad (2)$$

where:

$$k_x^2 + k_y^2 + k_z^2 = k_0^2 \quad (3)$$

k_x , k_y , and k_z correspond to the wave numbers in the x , y and z directions respectively. Plane wave behavior is the special case when $k_x = k_y = 0$.

Assuming the wall of the aperture is rigid, the boundary conditions are

$$\frac{\partial p}{\partial x} = 0 \text{ at } x = -a \text{ and } x = a \quad (4)$$

$$\frac{\partial p}{\partial y} = 0 \text{ at } y = -b \text{ and } y = b \quad (5)$$

Substituting Equations (4) and (5) into Equation (2) yields

$$C_3 = 1, \quad k_x = \frac{m\pi}{2a}, \quad m = 0, 1, 2, \dots \quad (6)$$

$$C_4 = 1, \quad k_y = \frac{n\pi}{2b}, \quad n = 0, 1, 2, \dots \quad (7)$$

Equation (2) becomes

$$p(x, y, z, t) = \sum_{m=0}^{\infty} \sum_{n=0}^{\infty} \cos\left(\frac{m\pi(x+a)}{2a}\right) \cos\left(\frac{n\pi(y+b)}{2b}\right) (C_{1,m,n} e^{-jk_{z,m,n}z} + C_{2,m,n} e^{+jk_{z,m,n}z}) e^{j\omega t} \quad (8)$$

where, from Equation (3), the transmission wave number for (m, n) mode, $k_{z,m,n}$, is given by

$$k_{z,m,n} = \left[k_0^2 - \left(\frac{m\pi}{2a}\right)^2 - \left(\frac{n\pi}{2b}\right)^2 \right]^{\frac{1}{2}} \quad (9)$$

The axial (z -component) particle velocity corresponding to the (m, n) mode can be determined using the momentum equation and can be expressed as

$$u_{z,m,n} = \frac{-\partial p / \partial z}{j\omega\rho_0} = \frac{k_{z,m,n}}{k_0\rho_0c_0} \cos\left(\frac{m\pi(x+a)}{2a}\right) \cos\left(\frac{n\pi(y+b)}{2b}\right) (C_{1,m,n}e^{-jk_{z,m,n}z} + C_{2,m,n}e^{+jk_{z,m,n}z})e^{j\omega t} \quad (10)$$

Any particular mode (m, n) will propagate unattenuated if $k_{z,m,n}$ is greater than zero. In that case,

$$k_{z,m,n} = \left[k_0^2 - \left(\frac{m\pi}{2a}\right)^2 - \left(\frac{n\pi}{2b}\right)^2 \right]^{\frac{1}{2}} > 0 \quad (11)$$

Obviously, a plane wave of any wavelength can propagate unattenuated, whereas a higher mode can propagate only insofar as Equation (11) is satisfied. Thus, if $b > a$, the cutoff frequency is

$$f_{cut} = \frac{c_0}{4b} \quad (12)$$

2.2 Force Equation at Incident Side

In order to predict the transmission loss for an aperture, the boundary conditions at the inlet and termination of the aperture must be accounted for properly. Similar to the authors' prior work (4), refer to Figure 2, the force equation on the incident side can be expressed as

$$(p_i + p_r) \iint_{S_1} \phi_{mn}(x, y) dS + p_s S_1 = p_1 S_1 \quad (13)$$

where p_i is the incident sound pressure, p_r is the reflected sound pressure, and $\phi_{mn}(x, y)$ is the mode shape of the (m, n) mode. The blocked sound pressure can be expressed as

$$\hat{p}_b = \hat{p}_i + \hat{p}_r = 2\hat{p}_i e^{-jk_0(\sin\theta_i \cos\phi_i x + \sin\theta_i \sin\phi_i y)} \cos(k_0 \cos\theta_i z) \quad (14)$$

The sound pressure inside the aperture on the incident side (p_1) can be expressed as

$$p_1 S_1 = \iint_{S_1} p_{0,mn} \phi_{mn}(x, y) \phi_{mn}(x, y) dS = p_{0,mn} \iint_{S_1} \phi_{mn}^2(x, y) dS \quad (15)$$

where S_1 is the cross-sectional area of the aperture. The scattered pressure (p_s) on the incident side can be expressed as

$$p_s S_1 = -\frac{S_1}{\hat{Z}_f \hat{k}_f} \sum_{p=0}^{\infty} \sum_{q=0}^{\infty} \hat{k}_{pq} u_{0,pq} \hat{Z}_{mnpq} \quad (16)$$

where \hat{Z}_f is the characteristic impedance inside the aperture, \hat{k}_f is the complex propagation constant, \hat{k}_{pq} is the wave number of the (p, q) mode, and \hat{Z}_{mnpq} is the cross modal radiation impedance between mode (m, n) and (p, q) .

Substituting Equation (14), (15) and (16) into Equation (13),

$$\begin{aligned} & 2\hat{p}_i e^{-jk_0(\sin\theta_i \cos\phi_i x + \sin\theta_i \sin\phi_i y)} \cos(k_0 \cos\theta_i z) \iint_{S_1} \phi_{mn}(x, y) dS \\ & = \frac{S_1}{\hat{Z}_f \hat{k}_f} \sum_{p=0}^{\infty} \sum_{q=0}^{\infty} \hat{k}_{pq} u_{0,pq} \hat{Z}_{mnpq} + p_{0,mn} \iint_{S_1} \phi_{mn}^2(x, y) dS \end{aligned} \quad (17)$$

Equation (17) describes the boundary condition for the incident side.

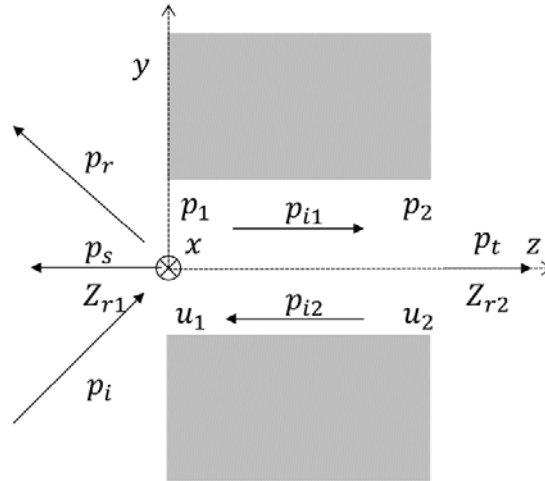


Figure 2 – Schematic representation of an aperture with the entry on the left and exit on the right.

2.3 Force Equation at Receiver Side

The other boundary condition is for the receiver side. The method is also similar to the authors' prior work (4). Referring to Figure 2, the equilibrium equation at receiver side is expressed as

$$p_2 S_2 = p_t S_2 \quad (18)$$

where p_2 is the sound pressure inside the aperture at the receiver side, p_t is the transmitted sound pressure, and S_2 is the cross-sectional area of the aperture on the receiver side. For the (m, n) mode,

$$p_2 S_2 = p_{l,mn} \iint_{S_2} \phi_{mn}^2(x, y) dS \quad (19)$$

$$p_t S_2 = \frac{S_2}{\hat{Z}_f \hat{k}_f} \sum_{p=0}^{\infty} \sum_{q=0}^{\infty} \hat{k}_{pq} u_{l,pq} \hat{Z}_{mnpq} \quad (20)$$

Substituting Equations (19) and (20) into Equation (18) yields

$$p_{l,mn} \iint_{S_2} \phi_{mn}^2(x, y) dS = \frac{S_2}{\hat{Z}_f \hat{k}_f} \sum_{p=0}^{\infty} \sum_{q=0}^{\infty} \hat{k}_{pq} u_{l,pq} \hat{Z}_{mnpq} \quad (21)$$

2.4 Transfer Matrix inside the Aperture

The wave propagation inside the aperture is similar to the wave propagating in a duct. The propagation equation for the (m, n) mode can be expressed as

$$p_{mn} = \hat{A}_{mn} e^{-jk_{mn}L} + \hat{B}_{mn} e^{jk_{mn}L} \quad (22)$$

$$u_{mn} = \hat{A}_{mn} e^{-jk_{mn}L} - \hat{B}_{mn} e^{jk_{mn}L} \quad (23)$$

at $z = 0$, p_{mn} and u_{mn} are:

$$p_{0,mn} = \hat{A}_{mn} + \hat{B}_{mn} \quad (24)$$

$$u_{0,mn} = \hat{A}_{mn} - \hat{B}_{mn} \quad (25)$$

at $z = l$, p_{mn} and u_{mn} are:

$$p_{l,mn} = \hat{A}_{mn} e^{-jk_{mn}l} + \hat{B}_{mn} e^{jk_{mn}l} \quad (26)$$

$$u_{l,mn} = \hat{A}_{mn} e^{-jk_{mn}l} - \hat{B}_{mn} e^{jk_{mn}l} \quad (27)$$

The transfer matrix for the (m, n) mode can be expressed as

$$\begin{Bmatrix} p_{0,mn} \\ u_{0,mn} \end{Bmatrix} = \begin{bmatrix} \cos(k_{z,mn}l) & j \sin(k_{z,mn}l) \\ j \sin(k_{z,mn}l) & \cos(k_{z,mn}l) \end{bmatrix} \begin{Bmatrix} p_{l,mn} \\ u_{l,mn} \end{Bmatrix} = \begin{bmatrix} A & B \\ C & D \end{bmatrix} \begin{Bmatrix} p_{l,mn} \\ u_{l,mn} \end{Bmatrix} \quad (28)$$

2.5 Derivation of TL

In order to determine TL of an aperture, the incident sound power and transmitted sound power must be described. According to Mechel (3), the incident sound power is

$$W_i = \frac{S_1}{2\rho_0 c_0} \cos \theta_i |\hat{p}_i|^2 \quad (29)$$

According to Sgard et al. (8), the transmitted sound power is

$$\begin{aligned} W_r &= \frac{1}{2} \operatorname{Re} \left(\int_{S_2} \hat{p}_2 \hat{u}_2^* dS \right) \\ &= \frac{1}{2} \operatorname{Re} \left(\frac{1}{Z_f k_f} \int_{S_2} \sum_{m=0}^{\infty} \sum_{n=0}^{\infty} p_{l,mn} \phi_{mn}(x, y) k_{mn} u_{l,mn}^* \phi_{mn}(x, y) dS \right) \\ &= \frac{1}{2} \operatorname{Re} \left(\frac{1}{Z_f k_f} \sum_{m=0}^{\infty} \sum_{n=0}^{\infty} p_{l,mn} k_{mn} u_{l,mn}^* \int_{S_2} \phi_{mn}^2(x, y) dS \right) \end{aligned} \quad (30)$$

Combining Equations (17), (21), (28), (29) and (30), and neglecting the cross modal radiation impedance ($m \neq p$ or $n \neq q$) which is very small, the sound transmission coefficient of an aperture with oblique incidence is expressed as

$$\begin{aligned} \tau(\theta_i, \varphi_i) &= \frac{W_r}{W_i} \\ &= \sum_{m=0}^{\infty} \sum_{n=0}^{\infty} \tau_{mn}(\theta_i, \varphi_i) \\ &= \sum_{m=0}^{\infty} \sum_{n=0}^{\infty} \frac{\rho_0 c}{\cos \theta_i} \left(\frac{k_{mn}}{Z_f k_f} \right)^2 \left| \frac{u_{l,mn}}{\hat{p}_i} \right|^2 \hat{Z}_{mnmn} \\ &= \sum_{m=0}^{\infty} \sum_{n=0}^{\infty} \frac{\rho_0 c}{\cos \theta_i} \left(\frac{k_{mn}}{Z_f k_f} \right)^2 \left| \frac{2F'_{mn}}{N_{mn}^2 (AZ_s + B + CZ_s^2 + DZ_s)} \right|^2 \hat{Z}_{mnmn} \end{aligned} \quad (31)$$

where

$$N_{mn}^2 = \iint_{S_1} \phi_{mn}^2(x, y) dS \quad (32)$$

$$F'_{mn} = \frac{\iint_{S_i} \hat{p}_b(x, y) \phi_{mn}(x, y) dS}{2 \hat{p}_i} \tag{33}$$

For a diffuse acoustic field, the transmission coefficient is expressed as

$$\tau_d = \frac{\int_0^{2\pi} \int_0^{\theta_{lim}} \tau(\theta_i, \varphi_i) \sin \theta_i \cos \theta_i d\theta_i d\varphi_i}{\pi \sin^2 \theta_{lim}} \tag{34}$$

and the transmission loss is expressed as

$$TL = -10 \log_{10}(\tau) \tag{35}$$

Note that Equations (31), (32), (33), (34) and (35) can be used for any cross-sectional shape.

3. EXAMPLES

3.1 Compared with Jiazhu et al. (4)

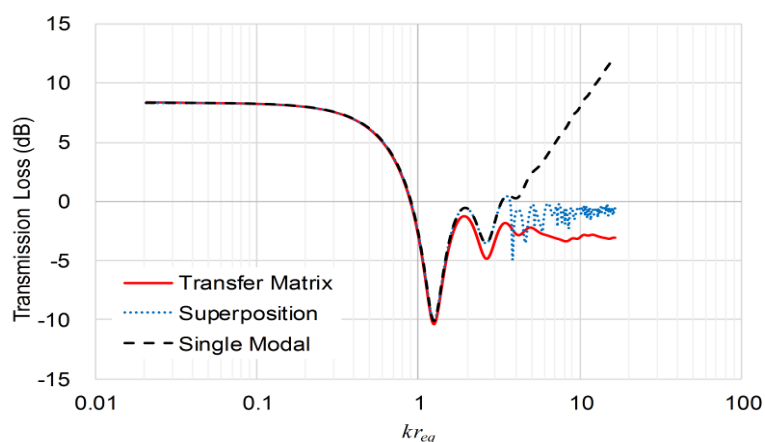


Figure 3 – Compared with Jiazhu et al. (4)
(Aperture size: $L_x = L_y = 100mm, L = 200mm$)

Figure 3 shows the comparison with the transfer matrix method. The cutoff frequency is approximately 1,700Hz. It can be seen that the result calculated by MSTCS approach agrees well with the transfer matrix method (4) up to the cutoff. In addition, the transmission loss results if only (0, 0) mode was used in the MSTCS method are shown. It can be seen that the transmission results are similar below the cutoff if only the first mode is considered. However, the transmission loss will be overly high above the cutoff frequency if higher order modes are not included.

3.2 Compared with Sgard et al. (8)

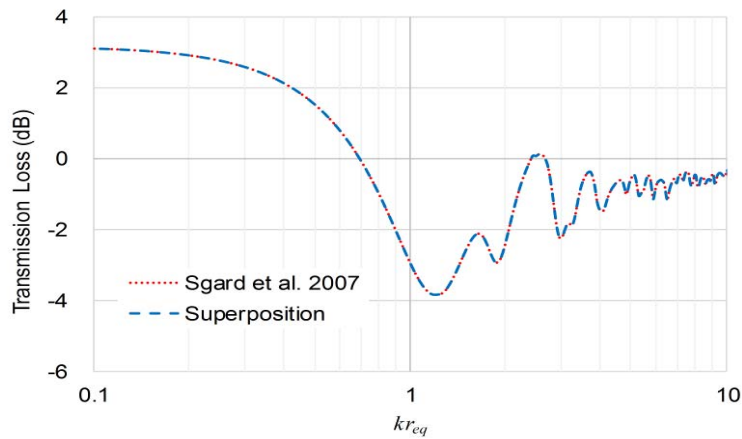


Figure 4 – Compared with Sgard et al. (8)

(Aperture size: $L_x = 400mm, L_y = 200mm, L = 200mm$)

Figure 4 shows that the results from MSTCS method and Sgard et al. are very close to each other. In this case the aperture cross-section was 400 mm x 200 mm, and the depth was 200 mm.

3.3 Compared with Trompette et al. (9)

Trompette et al. (9) determined the transmission loss of a number of apertures experimentally. Figure 5 compares results to Trompette et al. (9) for a 60 mm x 130 mm cross-section and a depth of 300 mm. Transmission loss results agree well.

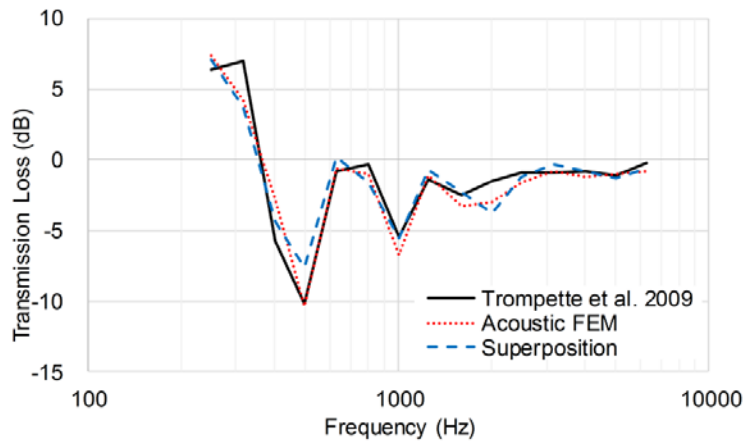


Figure 5 – Compared with Trompette at al. (9)

(Aperture size: $L_x = 60mm, L_y = 130mm, L = 300mm$)

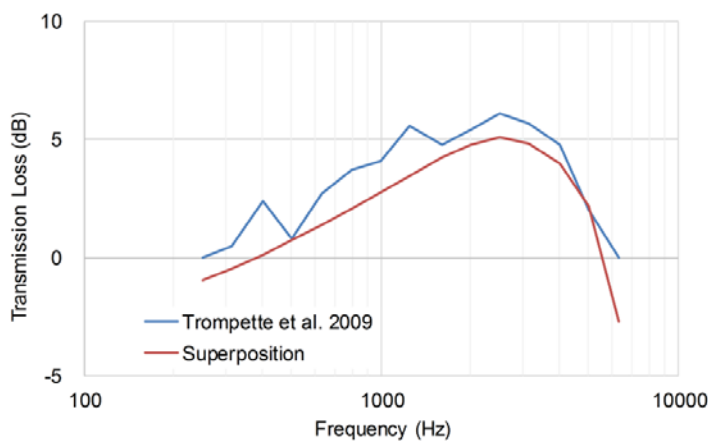


Figure 6 shows shows a similar result for a slit shape aperture.

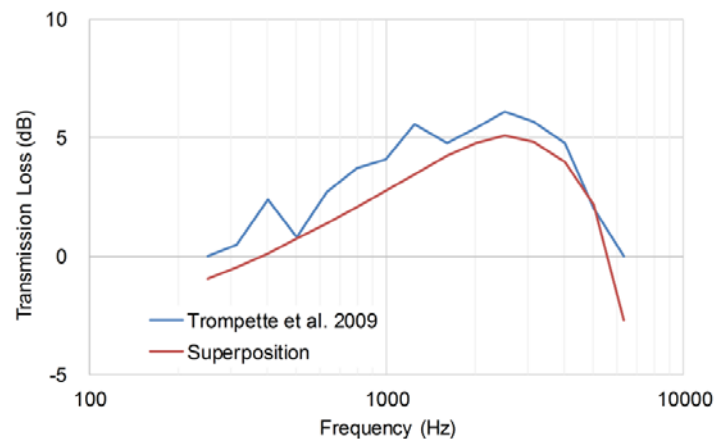


Figure 6 – Compared with Trompette at al. (9)
(Aperture size: $L_x = 500mm, L_y = 2mm, L = 1.5mm$)

4. CONCLUSIONS

In this paper, a modal and sound transmission coefficient superposition approach, similar to that developed by Sgard et al., but more efficient was used to determine the TL of apertures above the plane wave cutoff frequency. In the formulation described, the cross modal radiation impedance ($m \neq p$ or $n \neq q$) is neglected. The MSTCS method is applicable for oblique incident and diffuse acoustic fields and may be used for apertures having arbitrary cross-sections provided that the modes can be determined. MSTCS results were compared with those from Jiazhu et al. (4), Sgard et al. (8) and Trompette et al. (9) and agree well.

5. ACKNOWLEDGEMENTS

The authors gratefully acknowledge the support of the Vibro-Acoustics Consortium, the Chinese Scholarship Council. The authors are very grateful to Dr. Herrin, Professor Bi, Dr. Zhang and Dr. Lin who gave assistance.

REFERENCES

1. Ver IL, Beranek LL. *Noise and Vibration Control Engineering-Principles and Applications*. 2 ed. USA: Wiley; 2008. 966 p.
2. Gomperts MC. The "Sound Insulation" of Circular and Slit-shaped Apertures. *Acustica*. 1964;14(1):1-16.
3. Mechel FP. The acoustic sealing of holes and slits in walls. *Journal of Sound and Vibration*. 1986;111(2):5.
4. Li J, Zhou L, Hua X, Herrin DW. Transmission Loss of Variable Cross Section Apertures. *Journal of Vibration and Acoustics*. 2014;136(4):044501-5.
5. Gomperts MC, Kihlman T. Sound Transmission Loss of Circular and Slit-Shaped Apertures in Walls. *Acustica*. 1967;18(3):144-50.
6. Wilson GP, Soroka WW. Approximation to the Diffraction of Sound by a Circular Aperture in a Rigid Wall of Finite Thickness. *The Journal of the Acoustical Society of America*. 1965;37(2):286-97.
7. Sauter A, Soroka WW. Sound Transmission through Rectangular Slots of Finite Depth between Reverberant Rooms. *J Acoust Soc Am*. 1970;47(1p1):5-11.
8. Sgard F, Nelisse H, Atalla N. On the modeling of the diffuse field sound transmission loss of finite thickness apertures. *J Acoust Soc Am*. 2007;122(1):302-13.

9. Trompette N, Barbry J-L, Sgard F, Nelisse H. Sound transmission loss of rectangular and slit-shaped apertures: Experimental results and correlation with a modal model. *The Journal of the Acoustical Society of America*. 2009;125(1):31-41.
10. Sieck C, Lau S-K, editors. Noise propagation through open windows of finite depth into an enclosure. *Proceedings of Meetings on Acoustics*; 2012.
11. Poblet-Puig J, Rodríguez-Ferran A. Modal-based prediction of sound transmission through slits and openings between rooms. *Journal of Sound and Vibration*. 2013;332(5):1265-87.
12. Shorter PJ, Langley RS. Vibro-acoustic analysis of complex systems. *Journal of Sound and Vibration*. 2005;288(3):669-99.
13. Langley RS. Numerical evaluation of the acoustic radiation from planar structures with general baffle conditions using wavelets. *The Journal of the Acoustical Society of America*. 2007;121:766-77.
14. Langley RS. On the diffuse field reciprocity relationship and vibrational energy variance in a random subsystem at high frequencies. *J Acoust Soc Am*. 2007;121(2):913-21.
15. Herrin DW, Ramalingam S, Cui Z, Liu J. Predicting insertion loss of large duct systems above the plane wave cutoff frequency. *Applied Acoustics*. 2012;73(1):37-42.
16. ESI. VA-One Users Guide. USA: ESI Group; 2010. 596 p.
17. Munjal M. *Acoustics of Ducts and Mufflers*, 2nd edition. United Kingdom: John Wiley & Sons; 2014.